Open Access Library Journal
2026, Volume 13, e15866
ISSN Online: 2333-9721
ISSN Print: 2333-9705

Solid-Surface Fluorescence Determination of Samarium(III) Using an Eosin-o-Phenanthroline-HTAB System: Application to Water and Sediment Samples

Juan Manuel Pérez Iglesias[1], César Américo Almeida[1,2], María Carolina Talio[2,3*]

[1]Laboratory of Environmental Analytical Chemistry, Faculty of Chemistry, Biochemistry and Pharmacy, National University of San Luis, San Luis, Argentina
[2]Institute of Chemistry of San Luis (INQUISAL-CONICET), San Luis, Argentina
[3]Area of General and Inorganic Chemistry, Faculty of Chemistry, Biochemistry and Pharmacy, National University of San Luis, San Luis, Argentina
Email: *mctalio@unsl.edu.ar, *mcarolinatalio@gmail.com

How to cite this paper: Pérez Iglesias, J.M., Almeida, C.A. and Talio, M.C. (2026) Solid-Surface Fluorescence Determination of Samarium(III) Using an Eosin-o-Phenanthroline-HTAB System: Application to Water and Sediment Samples. *Open Access Library Journal*, **13**: e15866.
https://doi.org/10.4236/oalib.1115866

Received: August 8, 2026
Accepted: September 18, 2026
Published: September 21, 2026

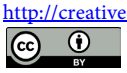

Abstract

Samarium is a technologically relevant rare earth element whose trace determination in aquatic systems requires sensitive and accessible analytical alternatives. A solid-surface fluorescence method was developed for Sm(III) using eosin, o-phenanthroline, hexadecyltrimethylammonium bromide (HTAB), and cellulose filter paper as the retention and measurement substrate. Experimental variables, including pH, reagent volumes, and the order of addition, were optimized. The selected sequence was eosin → o-phenanthroline → Sm(III) → HTAB → phosphate buffer, at pH 6.5. The retained system was measured at excitation/emission wavelengths of 525/645 nm. Fluorescence intensity was linear from 1.31 to 375.9 ng·L^{-1}, with R^2 = 0.9967. The calculated limits of detection and quantification were 0.39 and 1.31 ng·L^{-1}, respectively. No significant interference was observed for the investigated species at the tested molar ratios. Recoveries were 92.71% - 105.42% in natural waters and 99.50% - 100.43% in sediment extracts. Sm(III) was detected in six of ten water samples, while acid-extractable Sm concentrations in sediments ranged from 509.76 to 1218.68 μg·kg^{-1}. The aqueous fluorescence step avoided organic solvents and used small sample aliquots, low reagent concentrations, a cellulose support, and conventional instrumentation. These results demonstrate a simple and sensitive approach for Sm(III) screening in aquatic environmental samples, with potential advantages from a green analytical chemistry perspective that should be confirmed through formal assessment.

Subject Areas

Mineralogy

Keywords

Samarium(III), Solid-Surface Fluorescence, Filter Paper, Rare Earth Elements, Aquatic Samples, Green Analytical Chemistry

1. Introduction

Rare earth elements (REEs) are increasingly used in technological, electronic, energy, and industrial applications, raising interest in their occurrence and accumulation in aquatic environments. REEs have been reported in surface waters, sediments, and aquatic organisms under both natural and anthropogenic influences [1]-[4]. Their strong association with particulate matter, clays, organic matter, and Fe/Mn oxides makes sediments important sinks, while water reflects the dissolved or mobile fraction; therefore, both matrices provide complementary environmental information.

Samarium occurs predominantly as Sm^{3+} and can reach aquatic systems through weathering, sediment resuspension, industrial emissions, mining-related activities, and disposal of REE-containing materials. Although Sm-specific environmental information remains limited, adverse effects of individual REEs and REE mixtures have been reported for aquatic organisms [5] [6], supporting the need for sensitive methods suitable for trace-level determination in natural matrices.

ICP-MS is the reference technique for environmental REE determination because of its multielement capability and low detection limits. However, cost, specialized operation, sample preparation, and spectral or matrix interferences can limit routine use [7]. Complementary methods based on conventional molecular fluorescence instrumentation are therefore attractive for laboratories with more limited resources.

Sm^{3+} exhibits narrow 4f-4f emission bands, including the characteristic $^4G_5/_2 \rightarrow {}^6H_9/_2$ transition near 645 nm [8] [9]. Direct fluorescence is weak because 4f-4f absorption transitions are Laporte-forbidden, but complexation with aromatic ligands such as 1,10-phenanthroline can enhance the luminescent response [8] [9]. Eosin is an anionic xanthene dye whose fluorescence depends strongly on its microenvironment, while the cationic surfactant HTAB can interact electrostatically with eosin and promote organized ion-associated systems [10].

Previous work has shown that metal-1,10-phenanthroline-eosin systems can be retained and measured on cellulose filter paper [11]. Solid-surface fluorescence (SSF) is attractive because the substrate acts simultaneously as a retention and measurement support, potentially providing local preconcentration while reducing sample and reagent consumption. Filter paper is inexpensive and easy to han-

dle, although moisture, substrate heterogeneity, aggregation, and measurement geometry must be controlled [12] [13].

To our knowledge, eosin, 1,10-phenanthroline, and HTAB have not previously been combined with cellulose filter paper for SSF determination of Sm^{3+}. This study therefore develops and optimizes a Sm^{3+}-eosin-1,10-phenanthroline-HTAB SSF method, measured at λexc/λem = 525/645 nm, and evaluates its analytical performance and its application to natural waters and acid-extractable sediment fractions from San Luis, Argentina.

2. Materials and Methods

2.1. Reagents and Solutions

A certified Sm standard (1000 mg·L^{-1} in 2% HNO_3; CPI International, S4400-1000471) was diluted to obtain 1.0×10^{-3}, 1.0×10^{-6}, and 1.0×10^{-8} mol·L^{-1} Sm(III) solutions. Eosin (H.E. Daniel Ltd.) and o-phenanthroline (Merck) stock solutions were prepared at 1.0×10^{-3} mol·L^{-1}. Working solutions of both reagents at 1.0×10^{-7} mol·L^{-1} were subsequently prepared by serial dilution with ultrapure water. Under the optimized conditions, 250 µL of the eosin working solution and 1000 µL of the o-phenanthroline working solution were added to a final assay volume of 10.0 mL, corresponding to final concentrations of 2.5×10^{-9} and 1.0×10^{-8} mol·L^{-1}, respectively. HTAB (Sigma-Aldrich) was prepared at 1.0×10^{-2} mol·L^{-1} and diluted to a 1.0×10^{-3} mol·L^{-1} working solution. Potassium phosphate buffer (1.0×10^{-2} mol·L^{-1}) was adjusted with HCl or NaOH; optimized conditions were pH 6.5 and 2.0×10^{-4} mol·L^{-1} final phosphate. Blue-ribbon Whatman filter paper (2 - 5 µm, 4.5 cm diameter) was used as the SSF substrate. All reagents were analytical grade, and ultrapure water was used throughout.

2.2. Instrumentation

Fluorescence measurements were performed with a Shimadzu RF-5301 PC spectrofluorometer equipped with a 150 W xenon lamp and a solid-sample holder. Emission spectra were recorded from 500 to 750 nm at λexc = 525 nm; excitation/emission slit widths were 1.5/3.0 nm, and intensity at 645 nm was used for quantification. pH was measured with an Orion EA 940 analyzer.

2.3. General Solid-Surface Fluorescence Procedure

Calibration standards were prepared at 1.31, 15.04, 37.59, 75.18, 112.77, 150.36, 300.72, and 375.90 ng·L^{-1} Sm(III). A reagent blank was prepared separately and included as the zero-concentration level in the least-squares regression. Six independently prepared assay solutions were analyzed at each calibration level. Each solution was filtered through a separate cellulose paper substrate, air-dried, independently placed in the solid-sample holder, and measured under the selected instrumental conditions.

Intra-day precision was evaluated at 50 ng·L^{-1} using six independently prepared solutions analyzed on the same day. Inter-day precision was evaluated at the same

concentration by repeating six independent complete determinations on each of seven different days. Each determination included solution preparation, filtration through a separate cellulose substrate, drying, independent paper placement, and fluorescence measurement. Therefore, the reported precision represents the variability of the complete analytical procedure rather than repeated instrumental readings of the same substrate.

The complete solution was filtered through blue-ribbon cellulose paper, air-dried for 15 - 20 min until completely dry, and placed directly in the solid-sample holder. Emission was recorded at λexc = 525 nm, and the 645 nm signal was used as the analytical response. Samples followed the same procedure after the introduction of the water or sediment-extract aliquot.

Calibration standards were prepared at 1.31, 15.04, 37.59, 75.18, 112.77, 150.36, 300.72, and 375.90 ng·L^{-1} Sm(III). A reagent blank was prepared separately. The lowest calibration level, corresponding to the calculated LOQ of 1.31 ng·L^{-1}, was experimentally prepared and analyzed to verify its quantification performance.

2.4. Study Area and Sample Collection

In April 2026, paired water and sediment samples were collected upstream and downstream of five reservoirs in San Luis, Argentina: Dique Chico (M1-M2), Cruz de Piedra (M3-M4), Potrero de los Funes (M5-M6), La Estrechura (M7-M8), and Berta Vidal de Battini (M9-M10). Water was stored frozen in aliquots, and sediments were transported in resealable bags. Sampling coordinates were 33.300961˚S, 66.292621˚W (M1); 33.303872˚S, 66.316481˚W (M2); 33.256296˚S, 66.212217˚W (M3); 33.276033˚S, 66.228927˚W (M4); 33.220925˚S, 66.229500˚W (M5); 33.237842˚S, 66.239929˚W (M6); 33.208380˚S, 66.178012˚W (M7); 33.240606˚S, 66.179168˚W (M8); 33.163477˚S, 66.152481˚W (M9); and 33.171985˚S, 66.154498˚W (M10).

The closed Las Águilas East and West Ni-Cu-Co deposit is located approximately 4.8 - 5.7 km from M9-M10 and was considered only as a regional geological context, not evidence of direct mining input [14].

2.5. Water Sample Preparation and Analysis

Water samples were filtered through 0.45 μm syringe membranes. A 1.00 mL aliquot was transferred to a 10 mL flask and analyzed by the general SSF procedure. Accuracy and matrix effects were assessed by two-level spike-recovery experiments; native and spiked samples were measured six times (n = 6).

2.6. Sediment Sample Preparation and Analysis

Sediments were air-dried, ground, and sieved through a 2 mm mesh. Portions of 1.00 g of dry sediment were placed in digestion vessels and treated with 7.0 mL of concentrated HNO_3 (70%, v/v) and 3.0 mL of 10-volume H_2O_2. For the pre-digestion spike-recovery experiments, known amounts of Sm(III) standard solution were added directly to the digestion vessels after the addition of HNO_3 and H_2O_2

but before the heating step. Both spiked and unspiked samples were subsequently digested at 75˚C - 80˚C for 2 h.

After cooling, the extracts were quantitatively adjusted to 10.0 mL with ultrapure water, allowed to settle, and decanted. A 1.00 mL aliquot of each extract was diluted to 10.0 mL with ultrapure water and carefully neutralized with 0.10 mol·L^{-1} NaOH until a pH of approximately 6.0 was reached. Subsequently, 250 µL of the neutralized dilution was introduced into the 10.0 mL SSF assay. After the addition of all reagents and phosphate buffer, the pH of the complete assay solution was measured and confirmed to be approximately 6.0.

Samples whose concentrations exceeded the upper calibration limit of 375.9 ng·L^{-1} were further diluted, and the results were corrected using the corresponding dilution factor. The reported sediment concentrations represent the acid-extractable Sm fraction rather than the total Sm content. For each native and spiked extract, six independently prepared SSF assay solutions were analyzed on separate cellulose paper substrates, with independent paper placements.

3. Results and Discussion

3.1. Spectral Characteristics and Analytical Response

The retained Sm(III)-Eo-o-phen-HTAB system showed a concentration-dependent fluorescence increase at 645 nm (λexc = 525 nm), consistent with the characteristic $^4G_{5/2} \rightarrow {}^6H_{9/2}$ transition of Sm^{3+}. The blank intensity was 23 a.u., increasing to 981 a.u. at the highest calibration level (Figure 1(A)).

Regression of fluorescence intensity versus Sm(III) concentration gave IF = 378.85 CSm + 47.52 (CSm in 10^{-9} mol·L^{-1}), R^2 = 0.9967, over 1.31 - 375.9 ng·L^{-1} (Figure 1(B)).

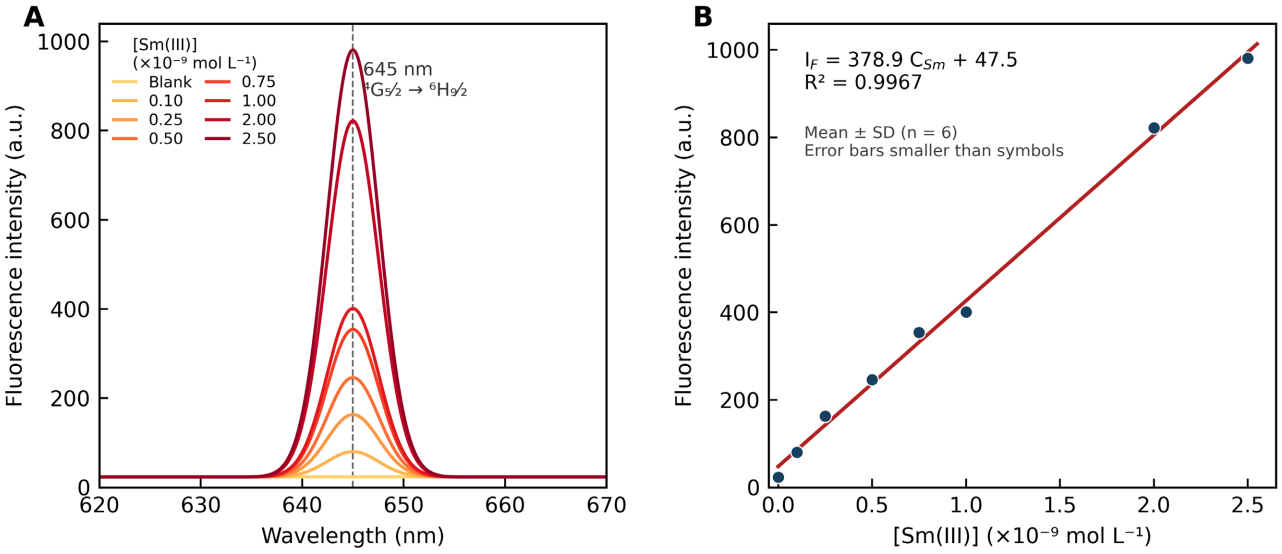

Figure 1. (A) Reconstructed solid-surface fluorescence emission profiles of the Sm(III)-Eo-o-phen-HTAB system at increasing Sm(III) concentrations. The profiles were generated using a common band shape centered at 645 nm and scaled to the experimental fluorescence intensity recorded at this wavelength. (B) Calibration plot obtained at λ_{exc} = 525 nm and λ_{em} = 645 nm.

3.2. Optimization of Experimental Variables

Effect of pH

Fluorescence increased from pH 4.0 to a maximum at pH 6.5 (640 a.u.), remained high between pH 6.0 and 7.5, and decreased at higher pH (Figure 2). Thus, pH 6.5 was selected. The trend may reflect changes in ligand protonation, Sm(III) hydrolysis, and retention of the fluorescent assembly; these mechanistic interpretations remain provisional because speciation was not independently evaluated.

Although pH 6.5 was selected as the optimum condition, the final sediment-assay solutions exhibited a pH of approximately 6.0 after neutralization and reagent addition. This value remained within the high-response interval observed between pH 6.0 and 7.5.

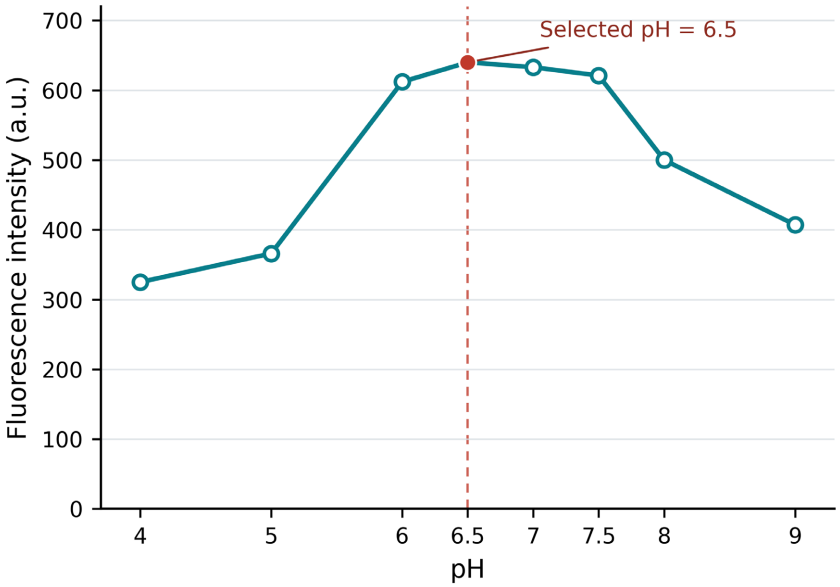

Figure 2. Effect of pH on the solid-surface fluorescence intensity of the Sm(III)-Eo-o-phen-HTAB system. Fluorescence measurements were performed at λexc = 525 nm and λem = 645 nm. Other experimental conditions were as described in Section 2.3.

Optimization of Ligand Volumes

Eosin and o-phenanthroline both enhanced the response (Figure 3). Eosin reached a plateau at 250 - 300 µL; 250 µL was selected as the minimum volume that provided maximum response. For o-phenanthroline, the maximum was obtained at 1000 µL, with no benefit at 1250 µL. These trends are consistent with ligand participation in the formation and sensitization of the retained fluorescent assembly, although stoichiometry was not independently established.

Effect of HTAB Volume

HTAB markedly enhanced fluorescence (Figure 4), increasing the signal from 254 a.u. without surfactant to 661 a.u. at 100 µL, an approximately 2.6-fold enhancement. Higher volumes produced no further improvement; therefore, 100 µL

was selected. The effect is consistent with favorable eosin-HTAB ion association and improved retention on cellulose, although aggregation/speciation was not independently studied.

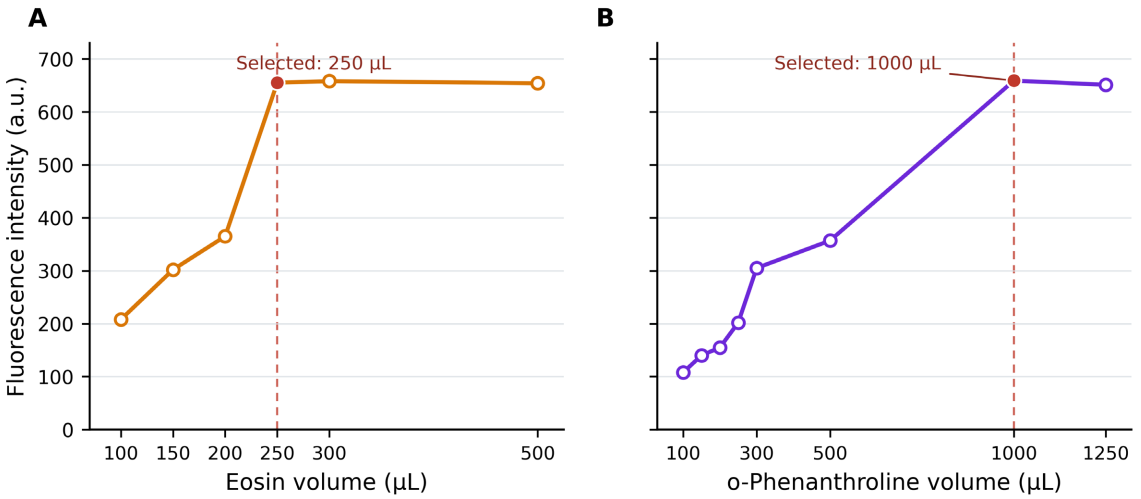

Figure 3. Influence of the added volumes of (A) eosin and (B) o-phenanthroline on the solid-surface fluorescence intensity of the Sm(III)-Eo-o-phen-HTAB system. Measurements were performed at λ_{exc} = 525 nm and λ_{em} = 645 nm. Other experimental conditions were as described in Section 2.3.

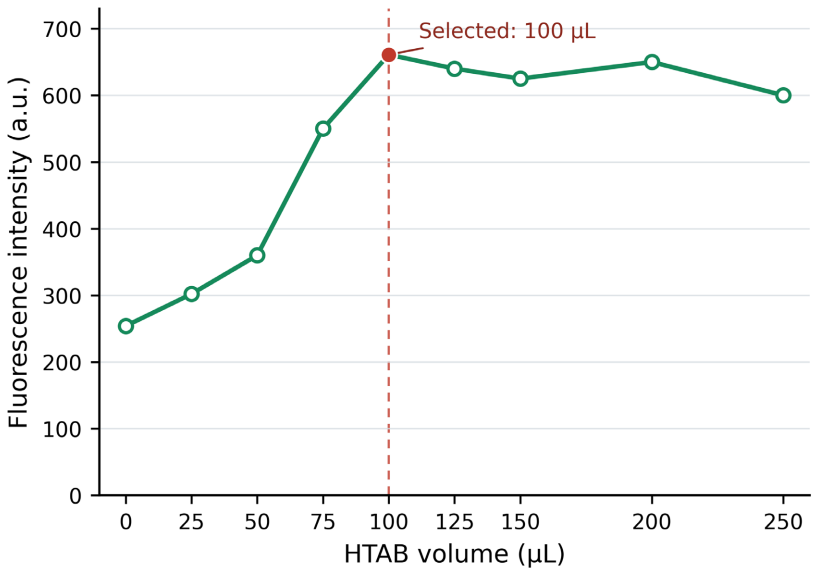

Figure 4. Effect of HTAB volume on the solid-surface fluorescence intensity of the Sm(III)-Eo-o-phen-HTAB system. Measurements were performed at λ_{exc} = 525 nm and λ_{em} = 645 nm. Other experimental conditions were as described in Section 2.3.

Effect of Phosphate Buffer Volume

Phosphate buffer volume affected the response (Figure 5): fluorescence increased from 347 a.u. at 100 µL to a maximum of 674 a.u. at 200 µL and then remained near a plateau. Accordingly, 200 µL was selected as the lowest volume providing maximum signal and adequate pH control.

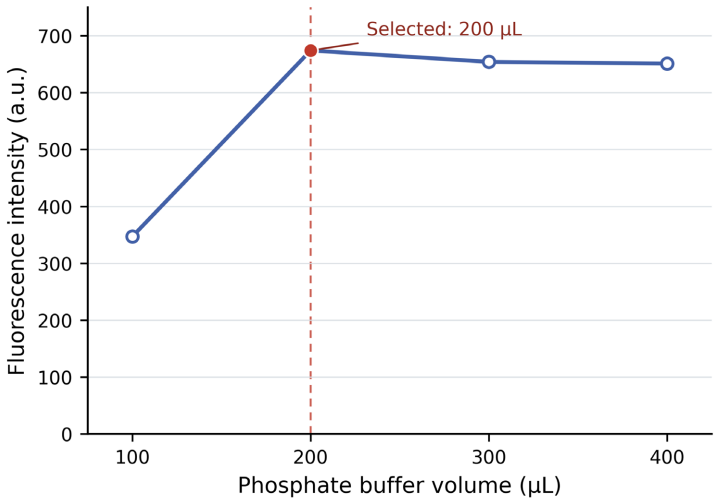

Figure 5. Effect of phosphate buffer volume on the solid-surface fluorescence intensity of the Sm(III)-Eo-o-phen-HTAB system. Measurements were performed at λ_{exc} = 525 nm and λ_{em} = 645 nm. Other experimental conditions were as described in Section 2.3.

Effect of Reagent Addition Order

The addition order strongly influenced fluorescence (**Figure 6**). The highest response (687 a.u.) was obtained for O1: Eo → o-phen → Sm(III) → HTAB → phosphate buffer. Alternative sequences gave lower signals, supporting ligand-metal association before surfactant organization and final pH adjustment. Because no kinetic or speciation study was performed, this interpretation remains provisional; O1 was adopted for subsequent measurements.

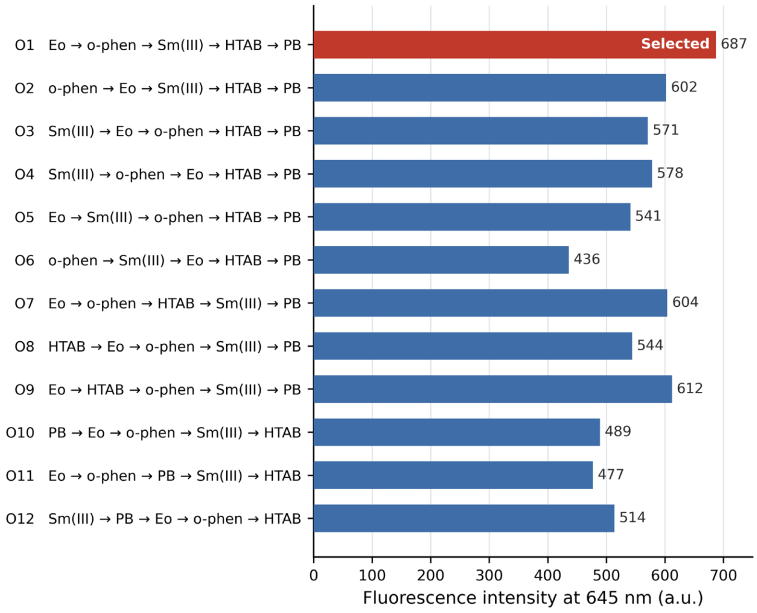

Figure 6. Effect of reagent addition order on the solid-surface fluorescence intensity of the Sm(III)-Eo-o-phen-HTAB system. PB: phosphate buffer. Measurements were performed at λ_{exc} = 525 nm and λ_{em} = 645 nm. Other experimental conditions were as described in Section 2.3.

3.3. Analytical Figures of Merit

Under the optimized conditions, the reagent blank and all Sm(III) calibration standards were included in the least-squares regression. The resulting calibration equation was (I_F = 378.85C_{Sm} + 47.52), where (C_{Sm}) is expressed in (10^{−9}) mol·L^{-1}, with (R^2 = 0.9967) over the range of 1.31 - 375.90 ng·L^{-1}. Six independently prepared assay solutions were analyzed at each calibration level. The RSD values obtained for the non-zero calibration levels ranged from 0.010 to 0.175%, while the standard deviation of the reagent blank was 0.33 a.u.

The LOD and LOQ, calculated as (3\sigma/slope) and (10\sigma/slope), were 0.39 and 1.31 ng·L^{-1}, respectively. The calculated LOQ was subsequently verified experimentally by preparing and analyzing Sm(III) solutions at 1.31 ng·L^{-1} under the complete SSF procedure. At this concentration, a mean recovery of 99.89% and an RSD of 0.21% were obtained, confirming that 1.31 ng·L^{-1} could be reliably quantified. Therefore, the experimentally verified linear range was 1.31 - 375.90 ng·L^{-1}.

Precision was evaluated at 50 ng·L^{-1} considering the complete analytical procedure. For intra-day precision, six independent solutions were prepared and individually filtered through six different cellulose substrates on the same day. Inter-day precision was assessed at the same concentration by performing six independent complete determinations on each of seven different days. Each substrate was independently dried, positioned in the solid-sample holder, and measured. The intra-day and inter-day RSD values were 0.33% and 0.36%, respectively. These results demonstrate satisfactory repeatability and intermediate precision, including variability associated with solution preparation, filtration, cellulose substrate heterogeneity, drying, paper placement, and instrumental measurement (See **Table 1**).

Table 1. Analytical performance of the proposed SSF method for Sm(III).

Parameter	Result
Linear range	1.31 - 375.90 ng·L^{-1}
Regression equation	IF = 378.85 CSm + 47.52
Coefficient of determination	R^2 = 0.9967
Reagent blank included in regression	Yes
Independent determinations per calibration level	6
Calibration sensitivity	378.85 a.u. per 10^{-9} mol·L^{-1}
SD of the reagent blank	0.33 a.u.
Calculated LOD	0.39 ng·L^{-1}
Calculated and experimentally verified LOQ	1.31 ng·L^{-1}
Recovery at the experimentally verified LOQ	99.89%
RSD at the experimentally verified LOQ	0.21%
Calibration-level RSD	0.010% - 0.175%
Intra-day precision at 50 ng·L^{-1}	0.33% (n = 6)
Inter-day precision at 50 ng·L^{-1}	0.36% (n = 6 per day; 7 days)

3.4. Interference Study for the Evaluated Species

The potential effects of selected cations, anions, and rare earth elements on the determination of Sm(III) were evaluated at a Sm(III) concentration of 1.0×10^{-9} mol·L^{-1}. The investigated species included Na^+, K^+, Ca^{2+}, Mg^{2+}, Al^{3+}, Fe^{3+}, Mn^{2+}, Co^{2+}, Ni^{2+}, Cu^{2+}, Zn^{2+}, Cd^{2+}, Pb^{2+}, Cr^{3+}, La^{3+}, Ce^{3+}, Nd^{3+}, Eu^{3+}, Gd^{3+}, Tb^{3+}, Cl^-, NO_3^-, SO_4^{2-}, CO_3^{2-}, HCO_3^-, and PO_4^{3-}. Each experimental condition was evaluated using six independently prepared solutions and separate cellulose paper substrates (n = 6). The results are reported as mean fluorescence intensity ± standard deviation and mean signal variation ± standard deviation (Table 2).

A signal variation of ±5% relative to the Sm(III) solution without interferent was adopted as the acceptance criterion. The evaluated species were tested at an interferent-to-Sm(III) molar ratio of 1000:1, except Cr(III), which was evaluated at 500:1. Mean signal variations ranged from −1.22% for Mg^{2+} to −0.15% for K^+ and Al^{3+}, while the associated standard deviations ranged from 0.09% to 0.21%. The standard deviations of the measured fluorescence intensities ranged from 2.04 to 2.34 a.u. None of the investigated species produced a signal variation exceeding the ±5% acceptance criterion under the tested conditions.

These results demonstrate satisfactory tolerance toward the specific ions and concentration ratios evaluated in this study. Because yttrium and the remaining lanthanides were not investigated, the results should not be interpreted as evidence of general selectivity against all rare earth elements.

Table 2. Effect of the evaluated potentially interfering species on the fluorescence determination of Sm(III). Results are expressed as mean ± SD based on six independent determinations.

Interfering Species	Interferent/Sm(III) Molar Ratio	Fluorescence Intensity (Mean ± SD, a.u.; n = 6)	Signal Variation (Mean ± SD, %; n = 6)
None	—	655.00 ± 2.11	—
Na^+	1000:1	651.00 ± 2.31	−0.61 ± 0.19
K^+	1000:1	654.00 ± 2.12	−0.15 ± 0.18
Ca^{2+}	1000:1	650.00 ± 2.18	−0.76 ± 0.14
Mg^{2+}	1000:1	647.00 ± 2.10	−1.22 ± 0.15
Al^{3+}	1000:1	654.00 ± 2.05	−0.15 ± 0.14
Fe^{3+}	1000:1	650.00 ± 2.06	−0.76 ± 0.13
Mn^{2+}	1000:1	652.00 ± 2.10	−0.46 ± 0.15
Co^{2+}	1000:1	653.00 ± 2.18	−0.31 ± 0.17
Ni^{2+}	1000:1	651.12 ± 2.21	−0.59 ± 0.19
Cu^{2+}	1000:1	650.14 ± 2.34	−0.74 ± 0.21
Zn^{2+}	1000:1	652.44 ± 2.13	−0.39 ± 0.18
Cd^{2+}	1000:1	653.01 ± 2.06	−0.30 ± 0.11
Pb^{2+}	1000:1	649.98 ± 2.05	−0.77 ± 0.12
Cr^{3+}	500:1	651.15 ± 2.10	−0.59 ± 0.15
La^{3+}	1000:1	650.77 ± 2.04	−0.65 ± 0.09

Continued

Ce^{3+}	1000:1	650.47 ± 2.14	−0.69 ± 0.12
Nd^{3+}	1000:1	651.23 ± 2.15	−0.58 ± 0.11
Eu^{3+}	1000:1	652.04 ± 2.12	−0.45 ± 0.17
Gd^{3+}	1000:1	650.76 ± 2.16	−0.65 ± 0.17
Tb^{3+}	1000:1	650.97 ± 2.20	−0.62 ± 0.18
Cl^-	1000:1	650.12 ± 2.18	−0.75 ± 0.21
NO_3^-	1000:1	649.85 ± 2.19	−0.79 ± 0.10
SO_4^{2-}	1000:1	649.37 ± 2.14	−0.86 ± 0.15
CO_3^{2-}	1000:1	651.55 ± 2.17	−0.53 ± 0.13
HCO_3^-	1000:1	651.24 ± 2.10	−0.57 ± 0.11
PO_4^{3-}	1000:1	650.17 ± 2.14	−0.74 ± 0.15

3.5. Application to Environmental Samples

Sediment Samples

Acid-extractable Sm(III) was quantified in all ten sediments (Table 3). Final analytical concentrations of 127.44 - 304.67 ng·L^{-1} corresponded to 509.76 - 1218.68 µg·kg^{-1} dry sediment after correction for extraction and dilution. M5 showed the lowest and M8 the highest value. These concentrations represent the acid-extractable fraction, not the absolute total Sm.

Pre-digestion spike recoveries ranged from 99.50% to 100.43%. Because the Sm(III) standard was added directly to the digestion vessels before heating, the spiked samples underwent the complete digestion and analytical procedure. These results therefore support satisfactory procedural recovery and limited matrix effects under the selected conditions.

Table 3. Determination of acid-extractable Sm(III) and pre-digestion spike-recovery results in sediment samples.

Sample	Sm(III) Found in Final Solution (ng·L^{-1})	Acid-Extractable Sm(III) in Dry Sediment (µg·kg^{-1})	Sm(III) Added (ng·L^{-1})	Sm(III) Found after Spiking (ng·L^{-1})	Recovery (%)
M1	302.12	1208.48	127	429.55	100.34
			255	557.01	99.96
M2	254.66	1018.64	127	381.95	100.23
			255	508.99	99.74
M3	245.87	983.48	127	372.55	99.75
			255	500.23	99.75
M4	301.23	1204.92	127	427.97	99.80
			255	556.57	100.13
M5	127.44	509.76	127	254.98	100.43
			255	382.04	99.84
M6	265.12	1060.48	127	391.87	99.80
			255	520.45	100.13

Continued

M7	297.66	1190.64	127	424.50	99.87
			255	553.01	100.14
M8	304.67	1218.68	127	431.04	99.50
			255	559.77	100.04
M9	204.55	818.20	127	331.23	99.75
			255	458.95	99.76
M10	209.47	837.88	127	336.88	100.32
			255	465.02	100.22

Natural Water Samples

Sm(III) was detected in six of ten natural waters; M3, M5, M6, and M9 were below the detection limit (Table 4). Detectable final-solution concentrations were 16.33 - 21.44 ng·L^{-1}, corresponding to 163.3 - 214.4 ng·L^{-1} in the original samples after the tenfold dilution correction. M4 had the lowest detectable concentration, and M8 the highest.

Spike recoveries in waters ranged from 92.71% to 105.42%, supporting satisfactory accuracy and limited matrix effects under the selected conditions.

Table 4. Determination of Sm(III) and spike-recovery results in natural water samples.

Sample	Sm(III) Found in Final Solution (ng·L^{-1})	Sm(III) in Original Water (ng·L^{-1})	Sm(III) Added (ng·L^{-1})	Sm(III) Found after Spiking (ng·L^{-1})	Recovery (%)
M1	20.22	202.2	17.7	37.90	99.89
			25.5	45.89	100.67
M2	19.25	192.5	17.7	35.66	92.71
			25.5	44.74	99.96
M3	ND	ND	17.7	17.87	100.96
			25.5	26.01	102.00
M4	16.33	163.3	17.7	34.45	102.37
			25.5	41.75	99.69
M5	ND	ND	17.7	17.81	100.62
			25.5	26.55	104.12
M6	ND	ND	17.7	17.57	99.27
			25.5	24.66	96.71
M7	17.33	173.3	17.7	35.23	101.13
			25.5	43.74	103.57
M8	21.44	214.4	17.7	40.10	105.42
			25.5	47.03	100.35
M9	ND	ND	17.7	17.75	100.28
			25.5	25.66	100.63
M10	17.45	174.5	17.7	35.10	99.72
			25.5	43.012	100.24

Accuracy Assessment and Validation Limitations

The accuracy of the proposed procedure was evaluated through two-level standard-addition and recovery experiments in all investigated water and sediment samples. For water samples, recoveries ranged from 92.71% to 105.42%, indicating satisfactory analyte recovery and limited matrix effects. For sediment samples, the Sm(III) standard was added directly to the digestion vessels before the heating step; therefore, the spiked samples underwent the complete digestion, dilution, neutralization, filtration, drying, and SSF measurement procedure. The corresponding pre-digestion recoveries ranged from 99.50% to 100.43%.

Additional evidence of method performance was provided by the experimentally verified LOQ, with a recovery of 99.89% and an RSD of 0.21%, as well as by intra-day and inter-day precision values of 0.33% and 0.36%, respectively. All calibration and spiking solutions were prepared from a certified 1000 $mg{\cdot}L^{-1}$ Sm standard solution.

Independent confirmation by ICP-MS or analysis of an appropriate certified reference material could not be performed during the present study. Therefore, the reported environmental concentrations should be interpreted as method-dependent estimates of the filtered Sm fraction in water and the acid-extractable Sm fraction in sediment. Although the standard-addition recoveries support the applicability of the procedure to the investigated matrices, future comparison with an independent reference technique or a suitable certified reference material would provide further confirmation of the method's accuracy.

4. Conclusion

A sensitive SSF method for Sm(III) was developed using eosin, o-phenanthroline, HTAB, and cellulose filter paper, with measurement at λexc/λem = 525/645 nm. The method was linear from 1.31 to 375.9 $ng{\cdot}L^{-1}$ (R^2 = 0.9967), with calculated LOD/LOQ values of 0.39/1.31 $ng{\cdot}L^{-1}$, good tolerance to the investigated interferents, and recoveries of 92.71% - 105.42% in waters and 99.50% - 100.43% in sediment extracts. Sm(III) was detected in six water samples, and the acid-extractable fraction was quantified in all sediments. The aqueous fluorescence step uses no organic solvent, small sample aliquots, low reagent concentrations, inexpensive cellulose, and conventional instrumentation. However, sediment pretreatment requires HNO_3/H_2O_2, and filter-paper waste is generated; a formal AGREE/BAGI assessment would therefore be appropriate before making broader greenness claims. Overall, the procedure provides a simple and accessible approach for screening and estimating filtered Sm in water and acid-extractable Sm in sediments. Independent validation using a reference technique or suitable certified reference material remains necessary before broader quantitative application.

Artificial Intelligence (AI) Use

The authors used ChatGPT (OpenAI) to assist with English-language editing, man-

uscript organization, and refinement of presentation. All AI-assisted content was critically reviewed and verified by the authors, who take full responsibility for the scientific content and the final version of the manuscript.

Author Contributions

Conceptualization: M.C.T. and J.M.P.I.; Methodology: M.C.T. and J.M.P.I.; Validation: J.M.P.I., C.A.A., and M.C.T.; Formal analysis: J.M.P.I. and M.C.T.; Investigation: J.M.P.I. and C.A.A.; Resources: M.C.T. and C.A.A.; Data curation: J.M.P.I. and M.C.T.; Writing—original draft preparation: J.M.P.I. and M.C.T.; Writing—review and editing: M.C.T., J.M.P.I. and C.A.A.; Visualization: J.M.P.I. and M.C.T.; Supervision: M.C.T.; Project administration: M.C.T.; Funding acquisition: M.C.T. All authors have read and agreed to the published version of the manuscript.

Funding

This work was supported by the research project PI UNSL No. 02-5226 "Application of Molecular Fluorescence Associated with Sensitization, Separation and Preconcentration Processes for the Monitoring of Emerging Contaminants Related to Human and Environmental Health" (Universidad Nacional de San Luis, UNSL, Argentina). Additional financial and institutional support was provided by the Consejo Nacional de Investigaciones Científicas y Técnicas (CONICET) and the Instituto de Química de San Luis (INQUISAL-CONICET), Argentina.

Data Availability

All data generated or analyzed during this study are included in this article. Additional information is available from the corresponding author upon reasonable request.

Acknowledgements

The authors gratefully acknowledge the financial and institutional support provided by the Universidad Nacional de San Luis (UNSL), the Consejo Nacional de Investigaciones Científicas y Técnicas (CONICET), and the Instituto de Química de San Luis (INQUISAL-CONICET).

Conflicts of Interest

The authors declare no competing interests.

References

[1] Marcinek, S., Grozdanić, O., Cindrić, A., Finderle, I. and Omanović, D. (2025) Rare Earth Elements and Yttrium in Seawater and Sediments of Contaminated Pula Bay. *Journal of Marine Science and Engineering*, **13**, Article 2338. https://doi.org/10.3390/jmse13122338

[2] Wang, S., Wang, Z., Gao, S., Zhang, X., Zeng, J. and Wu, Q. (2024) Rare Earth Elements in Lake Sediments Record Historic Environmental Influences from Anthropogenic Activities. *Ecological Indicators*, **159**, Article ID: 111680.

https://doi.org/10.1016/j.ecolind.2024.111680

[3] Pastorino, P., Squadrone, S., Berti, G., Esposito, G., Bondavalli, F., Renzi, M., *et al*. (2024) Occurrence of Rare Earth Elements in Water, Sediment, and Freshwater Fish of Diverse Trophic Levels and Feeding Ecology: Insights from the Po River (Northwest Italy). *Environmental Research*, **240**, Article ID: 117455. https://doi.org/10.1016/j.envres.2023.117455

[4] Ndjama, J., Mafany, G., Nkoue Ndondo, R.G., Belmond, B.E. and Ekoa Bessa, A.Z. (2022) Rare Earth Elements in Surface Waters and Sediments of the Mgoua Watershed, South Western Cameroon. *Arabian Journal of Geosciences*, **15**, Article No. 1001. https://doi.org/10.1007/s12517-022-10278-0

[5] Bergsten-Torralba, L.R., Magalhães, D.P., Giese, E.C., Nascimento, C.R.S., Pinho, J.V.A. and Buss, D.F. (2020) Toxicity of Three Rare Earth Elements, and Their Combinations to Algae, Microcrustaceans, and Fungi. *Ecotoxicology and Environmental Safety*, **201**, Article ID: 110795. https://doi.org/10.1016/j.ecoenv.2020.110795

[6] Hanana, H., Gagné, F., Trottier, S., Bouchard, P., Farley, G., Auclair, J., *et al*. (2022) Assessment of the Toxicity of a Mixture of Five Rare Earth Elements Found in Aquatic Ecosystems in Hydra Vulgaris. *Ecotoxicology and Environmental Safety*, **241**, Article ID: 113793. https://doi.org/10.1016/j.ecoenv.2022.113793

[7] Trommetter, G., Dumoulin, D. and Billon, G. (2020) Direct Determination of Rare Earth Elements in Natural Water and Digested Sediment Samples by Inductively Coupled Plasma Quadrupole Mass Spectrometry Using Collision Cell. *Spectrochimica Acta Part B: Atomic Spectroscopy*, **171**, Article ID: 105922. https://doi.org/10.1016/j.sab.2020.105922

[8] Ci, Y. and Lan, Z. (1989) Fluorometric Determination of Samarium and Gadolinium by Enhancement of Fluorescence of Samarium-Thenoyltrifluoroacetone-1,10-Phenanthroline Ternary Complex by Gadolinium. *Analytical Chemistry*, **61**, 1063-1069. https://doi.org/10.1021/ac00185a004

[9] Chauhan, A. and Langyan, R. (2021) Preparation, Characterization and Luminescence Behavior of Some Samarium Complexes. *Rare Metals*, **40**, 2618-2626. https://doi.org/10.1007/s12598-020-01552-9

[10] Acharya, S. and Rebery, B. (2009) Fluorescence Spectrometric Study of Eosin Yellow Dye-Surfactant Interactions. *Arabian Journal of Chemistry*, **2**, 7-12. https://doi.org/10.1016/j.arabjc.2009.07.010

[11] Talio, M.C., Acosta, M.G., Acosta, M., Olsina, R. and Fernández, L.P. (2015) Novel Method for Determination of Zinc Traces in Beverages and Water Samples by Solid Surface Fluorescence Using a Conventional Quartz Cuvette. *Food Chemistry*, **175**, 151-156. https://doi.org/10.1016/j.foodchem.2014.11.082

[12] Mamipour, Z. and Kompany-Zareh, M. (2024) A Solid-Surface Fluorescence Study of Rhodamine B and Fluorescein Adsorbed onto a Filter Paper, and Semi-Quantitative Determination Using EEM Data. *Journal of the Iranian Chemical Society*, **21**, 793-803. https://doi.org/10.1007/s13738-023-02961-0

[13] Nakaya, Y., Tomita, A. and Yamamura, H. (2024) Solid-Phase Fluorescence: Reproducibility and Comparison with the Solution States. *Talanta*, **270**, Article ID: 125566. https://doi.org/10.1016/j.talanta.2023.125566

[14] Servicio Geológico Minero Argentino (SEGEMAR) (2026) Base de Datos de Yacimientos Minerales de la República Argentina: Las Águilas Este y Oeste, deposit No. 11031. https://sigam.segemar.gov.ar/segedoc/res/img/sigam_yacimientos/dp11031.html